CMS Physics Analysis Summary

Contact: cms-pag-conveners-b2g@cern.ch 2014/03/12

Search for new physics with monotop final states in pp collisions at $\sqrt{s}$ = 8 TeV

The CMS Collaboration

Abstract

We perform a search for new physics in monotop final states, which contain a single top quark and large missing transverse energy induced by a weakly interacting massive particle. The measurement is performed using 19.7 fb^{-1} of $\sqrt{s} = 8$ TeV pp collision data, collected by the CMS detector at the LHC. No evidence of new physics is observed and exclusion limits on the mass of dark matter candidates are calculated at 95% Confidence Level. Scalar and vectorial dark matter particles with masses below 327 GeV and 655 GeV respectively, are excluded.

1 Introduction

Various models of new physics, such as universal extra dimensions [1] or supersymmetry [2, 3], predict the existence of new massive particles which are weakly interacting with matter. Such particles can be produced in collider experiments but escape detection and thus their existence can only be inferred by the presence of large missing transverse energy ($E_{\mathrm{T}}^{\mathrm{miss}}$). Both the ATLAS [4] and the CMS [5] collaborations have performed searches for monojet [6, 7] and monophoton [8, 9] signatures, which contain a single jet or a single photon associated with large $E_{\mathrm{T}}^{\mathrm{miss}}$. As no monojet nor monophoton events have been observed so far, it could be a sign that possible new particles favor coupling to massive Standard Model (SM) particles, such as the top quark. In this note, we present a search for monotop events, in which a potential dark matter (DM) particle is produced in association with a top quark [10–20].

The presented study focuses on the search for monotop signatures where a single top quark decays hadronically to a bottom quark and a W boson, which subsequently decays into a pair of light quarks. Large $E_{\mathrm{T}}^{\mathrm{miss}}$ originates from the dark matter candidate.

The search is based on 19.7 fb^{-1} of pp collision data at 8 TeV center-of-mass energy provided by the Large Hadron Collider (LHC) in 2012. The dominant Z+jets and W+jets backgrounds are estimated from data. The signal yield is determined simultaneously with the QCD multijet background, using a likelihood approach based on the observed multiplicity of b-tagged jets. We interpret the results within an effective field theory where the DM candidate can be a scalar or a vector boson. The simplest production mechanisms applicable for the both types of the DM candidate are shown in Fig. 1. In this work, we consider the case where the DM particle is produced by Flavor Changing Neutral Current (FCNC) diagrams.

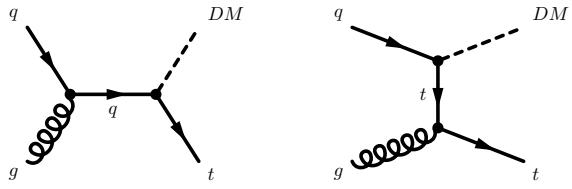

Figure 1: Feynman diagrams for s-channel (a) and t-channel (b) DM production.

2 Data and Simulated Samples

Data events are recorded using a trigger with a $E_{\mathrm{T}}^{\mathrm{miss}}$ threshold of 150 GeV. For the data-driven background estimate we use events with an isolated single muon trigger with a transverse momentum (p_{T}) threshold of 24 GeV.

The monotop model [21] is implemented within the FeynRules package [22, 23] and is interfaced [24, 25] with the MADGRAPH 5 event generator [26]. The coupling constants are set to 0.1, as suggested in [10]. The coupling constant affects only the cross section and not the kinematic properties of signal events. Simulated samples are produced for masses of DM particles varied from 0 to 1 TeV/c^2 in steps of 0.1 TeV/c^2. The production cross section at leading order (LO), as calculated by MADGRAPH with the CTEQ6.1L [27] Parton Density Functions (PDF), is given in Table 1. The production cross section for the vector DM scenario grows as $1/m^2$ for small mass DM candidate.

The leading SM background has three main components. One component arises from the $\mathrm{t\bar{t}}$

Table 1: Leading order production cross section of monotop events for scalar (middle column) and vector (right column) DM particles.

Mass (GeV)	$\sigma \times BR(t \to 3j)$(pb)	
	scalar DM	vector DM
1	6.320	184590
50	5.072	110.0
100	3.406	36.36
150	2.227	19.29
200	1.447	9.357
300	0.624	3.215
400	0.290	1.304
500	0.149	0.607
600	0.079	0.298
700	—	0.158
800	—	0.087
900	—	0.050
1000	—	0.030

and W+jets processes, where a charged lepton from W boson decay fails the selection or falls outside the detector acceptance. QCD multijet events, with mis-reconstructed jets inducing high $E_{\mathrm{T}}^{\mathrm{miss}}$, also contribute to the background. The only non-instrumental background arises from Z+3 jets events, with the Z boson decaying into a pair of neutrinos.

Most of the samples have been generated using MADGRAPH. For W+jets and Z+jets processes, parton-level events were generated including up to four additional partons. For the $\mathrm{Z}(\to \ell\ell|^{minv>50})$+jets and $\mathrm{W}(\to \ell\nu)$+jets processes we use the next-to-next-to-leading order (NNLO) cross sections of 3.504 nb and 37.509 nb respectively, as calculated by the FEWZ program [28]. For the $\mathrm{Z}(\to \nu\nu)$+jets process we use events generated in four bins of H_{T} (the scalar sum of p_{T} of all of the generated partons): $50 < H_{\mathrm{T}} < 100$ GeV, $100 < H_{\mathrm{T}} < 200$ GeV, $200 < H_{\mathrm{T}} < 400$ GeV, and $H_{\mathrm{T}} > 400$ GeV with LO cross sections of 381.2, 160.3, 41.49, and 5.274 pb respectively. Our $\mathrm{t\bar{t}}$ sample includes up to three additional partons at the matrix-element level, and events have been rescaled to an inclusive approximate NNLO cross section of 245.8 pb, as returned by the HATHOR package [29].

Additional sub-leading SM backgrounds are single top and di-boson production. Single top is modeled with POWHEG [30], and di-boson production is modeled with PYTHIA [31]. All Monte Carlo (MC) events are hadronized using PYTHIA 6.4.22 [31] and processed with a full simulation of the CMS detector implemented in the GEANT [32] package. A detailed description of the CMS detector can be found in [5].

3 Analysis Objects and Event Selection

We require at least one well-reconstructed primary vertex that is consistent with the beam spot position, and we veto non-collision backgrounds, such as events from beam halo or with a large detector noise.

The Particle Flow (PF) algorithm [33] is used to reconstruct and identify each particle with an optimized combination of information from all the CMS sub-detectors. Only the PF particles attached to the main primary vertex in the events are considered for the reconstruction. Other

PF particles are considered as originating from pile up (PU) events and are vetoed.

The signal selection requires large $E_{\mathrm{T}}^{\mathrm{miss}}$ and three jets from the hadronic decay of a top quark. Jets are reconstructed by an anti-k_T clustering algorithm [34] with a cone size of $\Delta R = 0.5$. Here $\Delta R = \sqrt{\Delta\eta^2 + \Delta\phi^2}$ with η being the pseudo-rapidity and ϕ being the azimuthal angle. During the jet reconstruction, the charged particles coming from PU events are excluded, while the neutral PU component is accounted for using the area-based procedure described in [35, 36]. Jet energy corrections used in this measurement rely on simulations and on studies performed with two-jet and photon+jet events in data [37]. Only jets with $p_{\mathrm{T}} \geq 35$ GeV and $|\eta| < 2.4$ are considered. The two leading jets must have a p_{T} above 60 GeV and the p_{T} of the third-jet has to be above 40 GeV. The invariant mass of the three jets has to be less than 250 GeV. Events containing additional jets with a p_{T} above 35 GeV are rejected. We require one of the three jets to be b-tagged by the Combined Secondary Vertex (CSV) b-tagging algorithm [38]. The CSV b-tagging algorithm is used with the medium working point, corresponding to a ∼70% efficiency to tag a b flavor jet and a probability of 1–4% to tag a light jet from u, d, and s quarks, or a gluon jet, calculated in $\mathrm{t\bar{t}}$ events. We also make use of events with zero b-tags in order to define a background-rich sample to extract the QCD background normalization.

For the signal selection, events with isolated muons or electrons are rejected. Muons are reconstructed by matching tracks from the outer muon detector to the tracks reconstructed by the inner tracker. The standard muon identification criteria [39] are applied. Loose muons are defined as muons satisfying $p_{\mathrm{T}} \geq 10$ GeV and $|\eta| < 2.4$. The electrons are reconstructed by associating tracks from the inner tracker with calorimetric clusters in the electromagnetic calorimeter. The standard electron identification criteria [40] are applied. Loose electrons are defined as electrons with $p_{\mathrm{T}} \geq 20$ GeV and within $|\eta| < 2.5$, excluding the transition region between barrel and end-cap defined by $1.444 < |\eta| < 1.566$. The muon (electron) isolation I_{rel} is computed by first summing the deposited energy of the reconstructed particles contained in a cone of $\Delta R = 0.4$ (0.3) around the muon (electron) direction, excluding the contribution of the lepton, and then dividing this sum by the transverse momentum of the lepton. The lepton candidates are rejected if they do not satisfy $I_{rel} < 0.2$.

For the off-line selection, the $E_{\mathrm{T}}^{\mathrm{miss}}$ is reconstructed as an absolute value of the negative vectorial sum of the transverse momenta of all of the reconstructed particles (charged and neutral) in the event. The $E_{\mathrm{T}}^{\mathrm{miss}}$ threshold is optimized to give the best expected limit and the $E_{\mathrm{T}}^{\mathrm{miss}}$ threshold of 350 GeV is chosen.

An alternative selection, requiring one or two isolated muons in addition to the three jets, is applied for a data-driven estimate of the W+jets and Z+jets backgrounds. For this, tighter selection is applied for muons. They are required to satisfy $p_{\mathrm{T}} \geq 40$ GeV and $|\eta| < 2.1$. The relative combined isolation in a cone of $\Delta R < 0.4$ must be below 0.12.

4 Signal and Background Estimates

The dominant backgrounds after the selection are $\mathrm{t\bar{t}}$ and V+jets events, with V being either Z or W bosons. An event signature with several jets is the natural final state for $\mathrm{t\bar{t}}$ production, with genuine $E_{\mathrm{T}}^{\mathrm{miss}}$ coming from neutrinos from leptonic W decays. The jets and $E_{\mathrm{T}}^{\mathrm{miss}}$ distributions in data $\mathrm{t\bar{t}}$ events are well reproduced by the simulation after applying the top quark p_{T} reweighting procedure presented in [41, 42]. Therefore, we rely on the simulation for the $\mathrm{t\bar{t}}$ background estimate. Other sub-dominant backgrounds, such as single-top quark and VV backgrounds, are also estimated from simulation.

For electroweak vector boson production, additional jets originate from QCD processes, which can lead to large systematic uncertainties when considering the production of up to three additional jets. For this reason, we choose to estimate the V+jets background contamination using data. The Z+jets background is determined by selecting Z($\rightarrow \mu\mu$)+jets events and replacing the $E_{\mathrm{T}}^{\mathrm{miss}}$ requirement by a requirement on the p_{T} of the di-muon pair, as will be discussed in Section 4.1. The W+jets background is estimated from the observed number of events passing a single muon selection using the probability for the muon to fail the lepton selection as it will be presented in Section 4.2. Events with isolated electrons have a noticeable contribution from the QCD processes and are not used for the V+jets background estimate.

While the $E_{\mathrm{T}}^{\mathrm{miss}}$ requirement effectively eliminates naturally balanced QCD multijet events, the overwhelming QCD production rate can still be a source of background events with large instrumental $E_{\mathrm{T}}^{\mathrm{miss}}$ coming from mis-reconstructed jets. As estimating such a background from simulation would entail very large uncertainties, due to imperfect description of mis-reconstruction effects by the simulation, we instead use b-tagging as a means to identify a multi-jet-enriched control region (events with zero b-tagged jets), and then we determine the QCD background yield from data.

4.1 Z+jets Background Estimate

The Z+jets event selection requires two isolated muons satisfying $p_{\mathrm{T}} \geq 40$ GeV and $|\eta| < 2.1$, and three jets with $p_{\mathrm{T}} \geq 60$, 60, and 40 GeV. Events with any additional jets with a p_{T} above 35 GeV are vetoed. Finally, we require the vectorial sum of p_{T} of di-muon pair and $E_{\mathrm{T}}^{\mathrm{miss}}$ to be above 350 GeV, the invariant mass of di-muon pair to be within 60–120 GeV range, and the invariant mass of the three jets to be less than 250 GeV.

The resulting di-muon yields are scaled to the di-neutrino yields with two factors: $R = BR(Z \rightarrow \nu\nu)/BR(Z \rightarrow \ell\ell) = 5.942$ [43], and acceptance$\times$efficiency ($A \times \epsilon$) to reconstruct the di-muon event in the detector. We estimate the yield of the Z($\rightarrow \nu\nu$)+jet background using the following equation:

$$N(Z \rightarrow \nu\nu) = \frac{N^{obs}(\mu\mu) - N^{MC}(non-Z)}{A \times \epsilon(\mu\mu)} \cdot \frac{BR(Z \rightarrow \nu\nu)}{BR(Z \rightarrow \mu\mu)} \quad (1)$$

where $N^{obs}(\mu\mu)$ is the observed number of di-muon events, and $N^{MC}(non-Z)$ is the number of non-Drell-Yan background events contributing to the di-muon sample, estimated from simulation. We observe 10 (1) di-muon events with zero (one) b-tagged jets. The non-Drell-Yan background is found to be negligible and the acceptance$\times$efficiency is measured in simulation to be 57$\pm$5%. This gives 103$\pm$34 (11$\pm$11) events with zero (one) b-tagged jets, to be compared to 89$\pm$88 (9$\pm$10) events predicted in simulation.

4.2 W+jets Background Estimate

We estimate the W+jets background using single muon events with $p_{\mathrm{T}} \geq 40$ GeV and $|\eta| < 2.1$. Events with any additional loose muons or electrons are vetoed. As for the Z+jets estimate, three jets with $p_{\mathrm{T}} \geq 60$, 60, and 40 GeV are required and events with any additional jets with p_{T} above 35 GeV are vetoed. Finally, we require $E_{\mathrm{T}}^{\mathrm{miss}}$ to be above 350 GeV, the invariant mass of the three jets to be less than 250 GeV, and the transverse mass of the muon and $E_{\mathrm{T}}^{\mathrm{miss}}$ to be less than 180 GeV.

W+jets events will not be removed by the explicit lepton veto of our selection if the lepton (electron or muon) is neither identified, nor isolated, nor within the acceptance region of the detector, or if the lepton is a hadronically decaying tau. A hadronically decaying prompt tau in simulated W+jets events yields an additional jet with $p_{\mathrm{T}} > 35$ GeV in 59$\pm$2% of the cases and

is removed by the jet cuts. In the remaining 41±2% of the cases the hadronic tau decays the W+jets background passes the signal selection.

The W+jets background for our signal selection can be estimated using:

$$N(W \to lost\ \ell\nu) = \frac{N^{obs}(\mu) - N^{MC}(non-W)}{A \times \epsilon(\mu)} \cdot \sum_{\ell=e,\mu,\tau} \frac{BR(W \to \ell\nu)}{BR(W \to \mu\nu)}\, p(lost\ \ell) \qquad (2)$$

where $N^{obs}(\mu)$ is the observed number of single muon events, $N^{MC}(non-W)$ is the number of non-W background events contributing to the single muon sample, estimated from simulation, $A \times \epsilon(\mu)$ is the probability to reconstruct, select, and identify an isolated muon, $p(lost\ e)$ and $p(lost\ \mu)$ are the probabilities for an electron or a muon to pass the loose-lepton veto, and $p(lost\ \tau)$ is the probability for a tau to decay hadronically and not be rejected by the jets selection. We observe 9 single muon events with zero b-tagged jets and expect 3.2±2 events of the non-W backgrounds. The $A \times \epsilon(\mu)$ and $p(lost\ \ell)$ terms are estimated in simulation. $A \times \epsilon(\mu)$ is found to be 30±5% while $p(lost\ e)$ and $p(lost\ \mu)$ are found to be 38±7% and 29±7% respectively. $p(lost\ \tau)$ is a product of 64.8% branching ratio of all hadronic tau decays and 41±2% probability for the W($\to \tau\nu \to hadrons\ \nu$)+jets event to pass the signal selection. Using all of the numbers in Eq.2 we obtain 18±12 W+jets background events with zero b-tagged jets, to be compared to 41±20 events in simulation.

In case of one b-tagged jet the W+jets production is suppressed and the absolute W+jets yield calculated with Eq. 2 is dominated by uncertainty from the non-W background simulation. We choose to normalize the W+jets rate with one b-tagged jet by scaling the rate with zero b-tagged jets by the probability to have a b-tagged jet in simulated W+jet event which is estimated to be 14.3±7.6%. This results in 2.6±2.2 W+jets background events with one b-tagged jets, to be compared to 3±2 events in simulation.

Table 2 shows the predicted number of events for signal, predicted backgrounds and data after the signal event selection.

Table 2: Standard Model backgrounds compared to data.

# of b tags	Z→ νν+jets	W+jets	$t\bar{t}$	Single top	VV	Sum	Data
zero b tags	103±34	18±12	5.9±4.5	2±0.5	5±0.4	134±36	143
one b tag	11±11	2.6±2.2	12±12	1±0.6	0±0	27±16	30

Figure 2 presents the distribution of the three-jet invariant mass. Good agreement between data and the background prediction is observed.

In Fig. 3 we compare the $E_{\mathrm{T}}^{\mathrm{miss}}$ spectrum in data and in the simulation. We apply the standard signal selection with the modified b tag requirement which helps us to validate the $t\bar{t}$ simulation and the V+jets simulation independently. The $t\bar{t}$ events are selected using additional requirement for two b-tagged jets. The V+jets event selection vetoes events with jets tagged by the CSV b-tagging algorithm at loose working point.

4.3 Signal extraction and QCD multijet background determination

The signal cross-section, as well as the number of QCD multijet background events, are measured in data using a likelihood approach, where each systematic source is treated as a nuisance parameters. The method is based on the observed number of events with zero and one b-tagged jets, accepted by the signal selection. These two event categories accumulate untagged and tagged signal and backgrounds events as shown in the following system of equations:

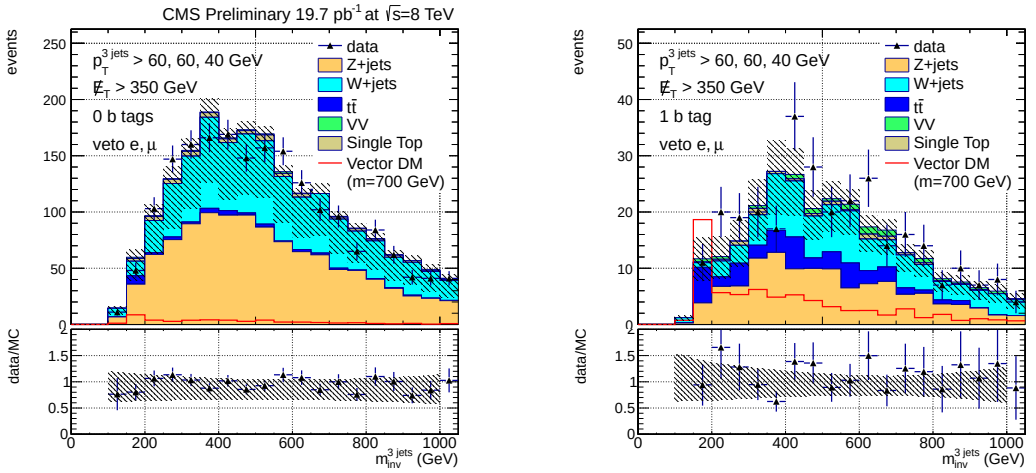

(a) (b)

Figure 2: The invariant mass of the three leading jets. In panels: (a) — zero b tags, (b) — one b tag. Measured distribution (points) are compared to the simulated backgrounds (stacked histograms) and one of the signal models (solid line) scaled to 19.7 fb^{-1}. The shaded area represents the square sum of the systematic uncertainties related to the renormalization and factorization scales for the $t\bar{t}$ and V+jets backgrounds.

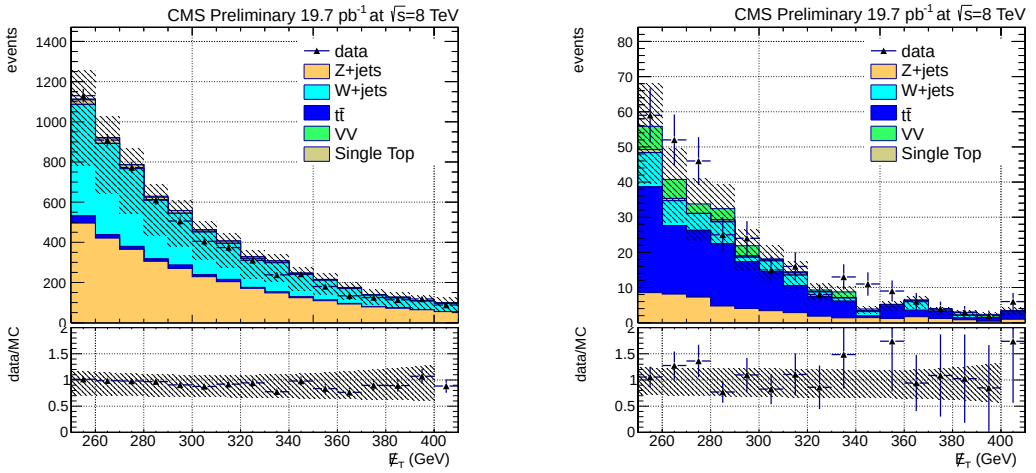

(a) (b)

Figure 3: $E_{\mathrm{T}}^{\mathrm{miss}}$ distribution in events after the signal selection with the modified b tag requirement. In panel (a) we use a b tag veto so as to enrich the sample with the V+jets events. In panel (b) we require two b tags so as to enrich the sample with $t\bar{t}$ events. The shaded area represents the square sum of the systematic uncertainties related to the renormalization and factorization scales for the $t\bar{t}$ and V+jets backgrounds.

$$\begin{cases} N^{0b} = p^{0b}_{sig} \cdot N_{sig} + p^{0b}_{QCD} \cdot N_{QCD} + N^{0b}_{other\ bg} \\ N^{1b} = p^{1b}_{sig} \cdot N_{sig} + p^{1b}_{QCD} \cdot N_{QCD} + N^{1b}_{other\ bg} \end{cases}, \tag{3}$$

where p^{0b}_{sig} and p^{1b}_{sig} are the probabilities to tag 0 or 1 jet as a b-jet in the selected signal events, p^{0b}_{QCD} and p^{1b}_{QCD} are the corresponding probabilities for the selected QCD events, and $N^{0b}_{other\ bg}$ and $N^{1b}_{other\ bg}$ are the known contributions to 0 and 1 b-tagged event categories from other backgrounds. The system above is solved to estimate the number of QCD (N_{QCD}) and signal (N_{sig}) events, by using a numerical minimization of the following likelihood :

$$\mathcal{L}_{\mathrm{S+B}}(\sigma_{sig}, \boldsymbol{\nu}) = Poisson\left(N^{0b}_{observed} | N^{0b}\right) \times Poisson\left(N^{1b}_{observed} | N^{1b}\right), \tag{4}$$

were σ_{sig} is the signal cross section (our parameter of interest), $\boldsymbol{\nu}$ is the vector of the nuisance parameters, and $N^{0b}_{observed}$ and $N^{1b}_{observed}$ are the total number of observed events in the zero-b-tags and one-b-tag event categories.

We derive the probabilities $p^{0b,1b}_{QCD}$, using QCD simulation. We select events with signal-like topology by vetoing loose leptons and requiring three jets satisfying $p_{\mathrm{T}} > 60$, 60 and 40 GeV. We further apply the $E^{\mathrm{miss}}_{\mathrm{T}}$ selection. The resulting probability to find one b-tagged jet in a simulated QCD event is found to be 18%. This value is consistent within 3% with the probability found using the QCD-enriched data events that are selected by the H_{T} trigger with a threshold of 250–550 GeV. So the value 18$\pm$3% is used in the analysis. The probability to not have any b-tagged jets in QCD simulation is 80$\pm$3%. The two probabilities are highly anti-correlated as only $\sim$ 2% of QCD events fall into the third category with two b-tagged jets. The result of this data-driven method for the QCD yield in our signal selection is consistent with 0 events. The $p^{0b,1b}_{QCD}$ and $p^{0b,1b}_{sig}$ numbers are summarized in Table 3.

Table 3: The $p^{0b,1b}_{QCD}$ and $p^{0b,1b}_{sig}$ parameters.

Parameter	p^{0b}_{QCD}	p^{1b}_{QCD}	p^{0b}_{sig}	p^{1b}_{sig}
Value	0.80	0.18	0.32	0.56
Uncertainty	0.03	0.03	0.05	0.05

5 Systematic Uncertainties

We estimate the systematic uncertainties in the simulation originating from the following sources. They are treated as nuisance parameters in the likelihood fit of Eq. 4.

Uncertainty on the jet energy scale is accounted for by varying the Jet Energy Corrections (JEC) within $\pm 1\sigma$ uncertainties and by varying the parameters for the Jet Energy Resolution (JER) smearing within their uncertainties [37]. These uncertainties are propagated to the $E^{\mathrm{miss}}_{\mathrm{T}}$ [37].

The b-tagging efficiency and mis-tagging rate scale-factors are measured in data and used to correct the performance of b-tagging in the simulation, including the correction of the shape of the CSV discriminator [38]. The scale factors are varied according to their $\pm 1\sigma$ uncertainties, and the propagated difference is assigned as a systematic uncertainty.

The systematics on the $t\bar{t}$ modeling, are introduced by using samples in which the matching thresholds and the renormalization and factorization scales are varied by a factor of 2. An additional uncertainty on the modeling of the top p_T spectra is estimated by reweighting the simulated top quark p_T to match the measured spectra [41, 42]. For all backgrounds estimated from simulation, we also account for uncertainties from the description of PDF, following the PDF4LHC recommendations [44].

The W+jets and Z+jets backgrounds are estimated from data and their uncertainties are used in the likelihood fit. These backgrounds are limited mostly by statistical uncertainty. All the systematic sources and the corresponding uncertainties are summarized in Table 4.

Table 4: Relative uncertainties on the signal and background yields for the signal selection with $E_{\mathrm{T}}^{\mathrm{miss}} > 350$ GeV. The last parameter, $N_{\mathtt{QCD}}$, is the absolute QCD yield, distributed uniformly in the given range.

nuisance parameter	$N_{\mathtt{S}}^{0b(1b)}$	$N_{t\bar{t}}^{0b(1b)}$	$N_{\mathtt{top}}^{0b(1b)}$	$N_{\mathtt{VV}}^{0b(1b)}$	$N_{\mathtt{W+jets}}^{0b(1b)}$	$N_{\mathtt{Z+jets}}^{0b(1b)}$	$N_{\mathtt{QCD}}$
$\mathcal{L}$	2.4%	2.4%	2.4%	2.4%	—	—	—
$E_{\mathrm{T}}^{\mathrm{miss}}$ trigger scale	1.4%	1.4%	1.4%	1.4%	—	—	—
$\mathrm{PDF}_{\mathtt{S}}$	$\lesssim 12\%$	—	—	—	—	—	—
$\mathrm{PDF}_{t\bar{t}}$	—	10(11)%	—	—	—	—	—
$\mathrm{PDF}_{\mathtt{top}}$	—	—	11(12)%	—	—	—	—
$\mathrm{PDF}_{\mathtt{VV}}$	—	—	—	6(8)%	—	—	—
JEC	$\lesssim 15\%$	14(22)%	44(56)%	7(25)%	—	—	—
JER	4(2)%	4(8)%	27(0)%	3(0)%	—	—	—
b tagging	6(2)%	10(15)%	0(0)%	2(14)%	—	—	—
Q^2-scale	—	35(76)%	—	—	—	—	—
$t\bar{t}$ matching	—	50(44)%	—	—	—	—	—
$t\bar{t}$ reweighting	—	41(41)%	—	—	—	—	—
Data-driven W+jets	—	—	—	—	67(85)%	—	—
Data-driven Z+jets	—	—	—	—	—	36(100)%	—
p_{QCD}^{1b}	—	—	—	—	—	—	17%
$N_{\mathtt{QCD}}$	—	—	—	—	—	—	0–10K

6 Results

The number of background events is compared to the data after the final event selection, as presented in Table 5. No excess above the SM background expectation is observed and limits at 95% Confidence Level (CL) are calculated. The limits are calculated using the CL_S technique [45–50] implemented within the ROOSTATS software package [51]. We choose the LHC-type full CL_S method [52]. This method utilizes the one-sided profile likelihood ratio test statistics and applies Frequentist treatment of nuisance parameters. The resulting limits are drawn using the expected signal yield and background yield prediction along with the systematic uncertainties for the both.

We use log-normal constraints for all of the uncertainties except for the uncertainties on the QCD and V+jets yields. The QCD yield is a free parameter assigned with a uniform probability. The Z+jets background yield is calculated the using number of observed di-muon events in the control region and the probability to accept and reconstruct a di-muon pair. Therefore, the Z+jets yield is constrained using a product of a Poisson probability to observe a given number

of di-muon events and a log-normal constraint on the acceptance times the reconstruction efficiency. Similarly, for the W+jets background we use a product of the Poisson probability to observe a given number of single muon events and log-normal constraints on all of the other parameters used in Eq. 2.

Table 5: Total number of selected events in data compared to the background prediction for $E_{\mathrm{T}}^{\mathrm{miss}} > 350$ GeV. The background yields are given with statistical (first) and systematic (second) uncertainties. Uncertainty on the simulated backgrounds ($t\bar{t}$, single top, and VV) are presented as a square sum of the uncertainties from all of the sources. The QCD background is calculated using all of the other backgrounds and data in Eq. 4. Uncertainty on the QCD background is 100% correlated with uncertainties on other backgrounds and therefore is dismissed. The final uncertainty on the sum of all backgrounds is the squre sum of uncertainties on all but QCD backgrounds.

# of b tags	Zero CSVm b tag	One CSVm b tag
$t\bar{t}$	$6\pm0\pm5$	$12\pm0\pm12$
W+jets	$18\pm9\pm7$	$3\pm1\pm2$
Z+jets	$103\pm33\pm9$	$11\pm10\pm1$
Single top	$2\pm1\pm1$	$1\pm1\pm1$
VV	$5\pm0\pm0$	$0\pm0\pm0$
QCD	6	1
sum	140 ± 36	28 ± 16
Data	143	30

Using the likelihood from equation 4 and nuisance parameters from Table 4, the best expected limit is obtained. In Fig. 4, we show the corresponding 95% C.L. expected and observed CL_S limits on the production cross section of the monotop DM candidate as a function of its mass.

7 Conclusion

We set limits on the monotop model which predicts the existence of scalar and vector dark matter candidates. The signature contains a single top quark decaying hadronically, and weakly interacting particles inducing missing transverse energy. The signal is extracted with the backgrounds using a likelihood based method. No excess of data over the SM prediction is found and exclusion limits are set at 95% Confidence Level. The observed lower limit for a scalar dark matter particle is 327 GeV, with an expected limit of $343^{+48,+79}_{-53,-109}$ GeV (for one- and two-σ bands). The observed lower limit for a vector dark matter particle is 655 GeV, with an expected limit of $668^{+39,+92}_{-48,-96}$ GeV. These results substantially improve previous limit on the monotop production published by the CDF collaboration [53].

References

[1] T. Appelquist, H.-C. Cheng, and B. A. Dobrescu, "Bounds on universal extra dimensions", *Phys.Rev.* **D64** (2001) 035002, doi:10.1103/PhysRevD.64.035002, arXiv:hep-ph/0012100.

[2] H. P. Nilles, "Supersymmetry, Supergravity and Particle Physics", *Phys.Rept.* **110** (1984) 1–162, doi:10.1016/0370-1573(84)90008-5.

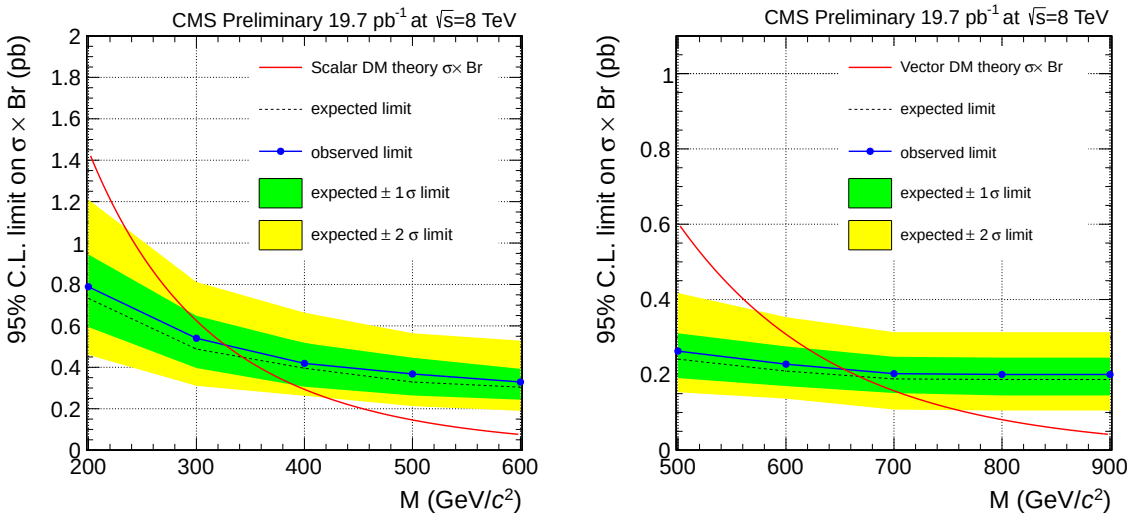

(a) (b)

Figure 4: The 95% C.L. expected and observed CL_S limits as a functions of the mass of the DM candidate. In panels: (a) — scalar DM model, (b) — vector DM model. The theory cross section is also shown with the red solid line.

[3] H. Haber and G. Kane, "The search for supersymmetry: Probing physics beyond the standard model", *Physics Reports* **117** (1985), no. 24, 75 – 263, doi:http://dx.doi.org/10.1016/0370-1573(85)90051-1.

[4] ATLAS Collaboration, "The ATLAS Experiment at the CERN Large Hadron Collider", *JINST* **3** (2008) S08003, doi:10.1088/1748-0221/3/08/S08003.

[5] CMS Collaboration, "The CMS experiment at the CERN LHC", *JINST* **3** (2008) S08004, doi:10.1088/1748-0221/3/08/S08004.

[6] ATLAS Collaboration, "Search for New Phenomena in Monojet plus Missing Transverse Momentum Final States using 10 fb^{-1} of pp Collisions at $\sqrt{s} = 8$ TeV with the ATLAS detector at the LHC", (2012).

[7] CMS Collaboration, "Search for dark matter and large extra dimensions in monojet events in pp collisions at $\sqrt{s} = 7$ TeV", *JHEP* **2012** (2012) 1–37, doi:10.1007/JHEP09(2012)094.

[8] ATLAS Collaboration, "Search for Dark Matter Candidates and Large Extra Dimensions in Events with a Photon and Missing Transverse Momentum in pp Collision Data at $\sqrt{s} = 7$ TeV with the ATLAS Detector", *Phys. Rev. Lett.* **110** (2013) 011802, doi:10.1103/PhysRevLett.110.011802.

[9] CMS Collaboration, "Search for Dark Matter and Large Extra Dimensions in pp Collisions Yielding a Photon and Missing Transverse Energy", *Phys. Rev. Lett.* **108** (2012) 261803, doi:10.1103/PhysRevLett.108.261803.

[10] J. Andrea, B. Fuks, and F. Maltoni, "Monotops at the LHC", *Phys.Rev.* **D84** (2011) 074025, doi:10.1103/PhysRevD.84.074025, arXiv:1106.6199.

[11] J.-L. Agram et al., "Monotop phenomenology at the Large Hadron Collider", *Phys.Rev.* **D89** (2014) 014028, doi:10.1103/PhysRevD.89.014028, arXiv:1311.6478.

[12] F. del Aguila, J. Aguilar-Saavedra, and L. Ametller, "Z t and gamma t production via top flavor changing neutral couplings at the Fermilab Tevatron", *Phys.Lett.* **B462** (1999) 310–318, doi:10.1016/S0370-2693(99)00929-6, arXiv:hep-ph/9906462.

[13] D. Morrissey, T. M. Tait, and C. Wagner, "Proton lifetime and baryon number violating signatures at the CERN LHC in gauge extended models", *Phys.Rev.* **D72** (2005) 095003, doi:10.1103/PhysRevD.72.095003, arXiv:hep-ph/0508123.

[14] N. Desai and B. Mukhopadhyaya, "R-parity violating resonant stop production at the Large Hadron Collider", *JHEP* **1010** (2010) 060, doi:10.1007/JHEP10(2010)060, arXiv:1002.2339.

[15] Z. Dong et al., "Baryon number violation at the LHC: the top option", *Phys.Rev.* **D85** (2012) 016006, doi:10.1103/PhysRevD.85.016006,10.1103/PhysRevD.85.039907, arXiv:1107.3805.

[16] H. Davoudiasl, D. E. Morrissey, K. Sigurdson, and S. Tulin, "Baryon Destruction by Asymmetric Dark Matter", *Phys.Rev.* **D84** (2011) 096008, doi:10.1103/PhysRevD.84.096008, arXiv:1106.4320.

[17] J. Wang, C. S. Li, D. Y. Shao, and H. Zhang, "Search for the signal of monotop production at the early LHC", *Phys.Rev.* **D86** (2012) 034008, doi:10.1103/PhysRevD.86.034008, arXiv:1109.5963.

[18] J. F. Kamenik and J. Zupan, "Discovering Dark Matter Through Flavor Violation at the LHC", *Phys.Rev.* **D84** (2011) 111502, doi:10.1103/PhysRevD.84.111502, arXiv:1107.0623.

[19] E. Alvarez, E. C. Leskow, J. Drobnak, and J. F. Kamenik, "Leptonic Monotops at LHC", *Phys.Rev.* **D89** (2014) 014016, doi:10.1103/PhysRevD.89.014016, arXiv:1310.7600.

[20] A. Kumar, J. N. Ng, A. Spray, and P. T. Winslow, "Tracking Down the Top Quark Forward-Backward Asymmetry with Monotops", *Phys.Rev.* **D88** (2013) 075012, doi:10.1103/PhysRevD.88.075012, arXiv:1308.3712.

[21] "Monotop web repository: http://feynrules.irmp.ucl.ac.be/wiki/Monotops",.

[22] N. D. Christensen and C. Duhr, "FeynRules - Feynman rules made easy", *Comput.Phys.Commun.* **180** (2009) 1614–1641, doi:10.1016/j.cpc.2009.02.018, arXiv:0806.4194.

[23] A. Alloul et al., "FeynRules 2.0 - A complete toolbox for tree-level phenomenology", arXiv:1310.1921.

[24] N. D. Christensen et al., "A Comprehensive approach to new physics simulations", *Eur.Phys.J.* **C71** (2011) 1541, doi:10.1140/epjc/s10052-011-1541-5, arXiv:0906.2474.

[25] C. Degrande et al., "UFO - The Universal FeynRules Output", *Comput.Phys.Commun.* **183** (2012) 1201–1214, doi:10.1016/j.cpc.2012.01.022, arXiv:1108.2040.

[26] J. Alwall et al., "MadGraph 5 : Going Beyond", *JHEP* **1106** (2011) 128, doi:10.1007/JHEP06(2011)128, arXiv:1106.0522.

[27] J. Pumplin et al., "New generation of parton distributions with uncertainties from global QCD analysis", *JHEP* **0207** (2002) 012, doi:10.1088/1126-6708/2002/07/012, arXiv:hep-ph/0201195.

[28] K. Melnikov and F. Petriello, "Electroweak gauge boson production at hadron colliders through $O(\alpha_s^2)$", *Phys. Rev. D* **74** (2006) 114017, doi:10.1103/PhysRevD.74.114017, arXiv:hep-ph/0609070.

[29] M. Aliev et al., "HATHOR: HAdronic Top and Heavy quarks crOss section calculatoR", *Comput.Phys.Commun.* **182** (2011) 1034–1046, doi:10.1016/j.cpc.2010.12.040.

[30] S. Frixione, P. Nason, and C. Oleari, "Matching NLO QCD computations with parton shower simulations: the POWHEG method", *JHEP* **11** (2007) 070, doi:10.1088/1126-6708/2007/11/070, arXiv:0709.2092.

[31] T. Sjöstrand, S. Mrenna, and P. Z. Skands, "PYTHIA 6.4 Physics and Manual", *JHEP* **05** (2006) 026, doi:10.1088/1126-6708/2006/05/026, arXiv:hep-ph/0603175.

[32] GEANT4 Collaboration, "GEANT4: A simulation toolkit", *Nucl. Instrum. Meth.* **A506** (2003) 250–303, doi:10.1016/S0168-9002(03)01368-8.

[33] CMS Collaboration, "Particle Flow Event Reconstruction in CMS and Performance for Jets, Taus, and MET", CMS Physics Analysis Summary CMS PAS-PFT-2009/001.

[34] M. Cacciari, G. Salam, and G. Soyez, "The Anti-k_T Jet Clustering Algorithm", *JHEP* **04** (2008) 063, doi:10.1088/1126-6708/2008/04/063.

[35] M. Cacciari, G. P. Salam, and G. Soyez, "FastJet User Manual", *Eur. Phys. J. C* **72** (2012) 1896, doi:10.1140/epjc/s10052-012-1896-2, arXiv:1111.6097.

[36] M. Cacciari and G. P. Salam, "Dispelling the N^3 myth for the k_t jet-finder", *Phys. Lett. B* **641** (2006) 57–61, doi:10.1016/j.physletb.2006.08.037, arXiv:hep-ph/0512210.

[37] CMS Collaboration, "Determination of the Jet Energy Scale in CMS with pp Collisions at $\sqrt{s} = 7$ TeV", CMS Physics Analysis Summary CMS-PAS-JME-10-010, 2010.

[38] CMS Collaboration, "Identification of b-quark jets with the CMS experiment", arXiv:1211.4462.

[39] "Performance of muon identification in pp collisions at $\sqrt{s} = 7$ TeV", Technical Report CMS-PAS-MUO-10-002, CERN, 2010. Geneva, 2010.

[40] "Electron reconstruction and identification at $\sqrt{s} = 7$ TeV", Technical Report CMS-PAS-EGM-10-004, CERN, Geneva, 2010.

[41] CMS Collaboration, "Measurement of differential top-quark pair production cross sections in the lepton+jets channel in pp collisions at 8 TeV", Technical Report CMS-PAS-TOP-12-027, CERN, Geneva, 2013.

[42] CMS Collaboration, "Measurement of the differential ttbar cross section in the dilepton channel at 8 TeV", Technical Report CMS-PAS-TOP-12-028, CERN, Geneva, 2013.

[43] Particle Data Group Collaboration, "Review of particle physics", *J. Phys.* **G37** (2010) 075021, doi:10.1088/0954-3899/37/7A/075021.

[44] PDF4LHC Collaboration, "Practical implementation of the PDF4LHC recipe", technical report.

[45] A. L. Read, "Presentation of search results: the CLs technique", *J. Phys. G* **G28** (2002) 2693–2704, doi:10.1088/0954-3899/28/10/313.

[46] A. L. Read, "Modified frequentist analysis of search results (the CLs method)", *Proceedings of the First Workshop on Confidence Limits, CERN, Geneva, Switzerland* (2000).

[47] T. Junk, "Confidence level computation for combining searches with small statistics", *Nucl. Instrum. Meth.* **A434** (1999) 435, doi:10.1016/S0168-9002(99)00498-2.

[48] W. Fisher, "Collie: A confidence level limit evaluator", D0 Note 5595, 2009.

[49] W. Fisher, "Systematics and limit calculations", *FERMILAB-TM-2386-E* **A434** (2006) doi:10.2172/923070.

[50] T. Junk, "Sensitivity, Exclusion and Discovery with Small Signals, Large Backgrounds, and Large Systematic Uncertainties.", CDF/DOC/STATISTICS/PUBLIC 8128, 2007.

[51] L. Moneta et al., "The RooStats Project", in *13^{th} International Workshop on Advanced Computing and Analysis Techniques in Physics Research (ACAT2010)*. SISSA, 2010. arXiv:1009.1003. PoS(ACAT2010)057.

[52] ATLAS and CMS Collaborations, "Procedure for the LHC Higgs boson search combination in Summer 2011", *CERN Document Server* (2011), no. CMS-NOTE-2011-005,.

[53] CDF Collaboration, "Search for a dark matter candidate produced in association with a single top quark in $p\bar{p}$ collisions at $\sqrt{s} = 1.96$ TeV", *Phys.Rev.Lett.* **108** (2012) 201802, doi:10.1103/PhysRevLett.108.201802, arXiv:1202.5653.